Spectroscopy and Reactivity of Kekulé Hydrocarbons with Very Small Singlet−Triplet Gaps

Daniel R. McMasters*,† and Jakob Wirz

Contribution from the Institut für Physikalische Chemie der Universität Basel, Klingelbergstrasse 80, CH-4056 Basel, Switzerland

Received February 4, 2000. Revised Manuscript Received October 2, 2000

Abstract: Two Kekulé hydrocarbons, 2,2-dimethyl-2*H*-benzo[*cd*]fluoranthene (**1**) and its benzannellated analogue 2,2-dimethyl-2*H*-dibenzo[*cd,k*]fluoranthene (**2**), were generated photochemically from two different photoprecursors each and investigated spectroscopically in cryogenic matrices by UV−vis, fluorescence, and EPR and in solution using ns flash photolysis and chemical trapping experiments. Hydrocarbon **1** is a ground-state singlet species, whereas compound **2** has a triplet ground state, the first such neutral Kekulé hydrocarbon. This difference, which is supported by density functional calculations, has profound influence on the spectroscopy and reactivity of the two compounds. Using the results of the spectroscopic measurements, trapping experiments, and density functional calculations, the singlet−triplet gap for **1** is estimated to be 2.3−2.8 kcal mol^{-1}, with the singlet the ground state, and 0.8−1.3 kcal mol^{-1} for **2**, in favor of the triplet.

Introduction

For much of the twentieth century, it was thought that any molecule possessing a fully bonding resonance structure will exist as ground-state singlet species, that is, that only non-Kekulé molecules, whose topologies preclude bonding among all π centers, are triplet diradicals in the ground state. The preference for the triplet state in molecules with degenerate frontier orbitals, however, suggested the possibility that molecules with a sufficiently small energy gap between the highest occupied molecular orbital (HOMO) and the lowest unoccupied molecular orbital (LUMO) would also exist as triplets in the ground state, a hypothesis formulated by Longuet-Higgins in 1950.[1] The theory was refined by Hoffmann in 1968,[2] who proposed an estimate of the threshold HOMO−LUMO gap.

Specific examples of possible exceptions to the classical model were first proposed in the 1960s based on the results of Pariser−Pople−Parr (PPP) calculations. The PPP model allowed the estimation of excited-state energies for large molecules and was applied to numerous hydrocarbons of various topologies. Among the compounds which have been proposed as candidate ground-state triplet Kekulé hydrocarbons are cyclohepta[*def*]-fluorene,[3] anthracene-2,3-dimethylene,[4] nonacene and longer linear acenes,[5,6] cyclohepta[*a*]cyclopenta[*i*]anthracene,[7,8] and pleiadene and benzopleiadene.[9−12]

Previous studies of quinonoid hydrocarbons indicate that an extremely small HOMO−LUMO gap is necessary to stabilize the triplet state to the point that it becomes the ground state. One possibility for decreasing the HOMO−LUMO gap would be to extend the linear acene or *o*-xylylene series. However, very low HOMO−LUMO splittings are observed only for relatively large members of this series. This would make the synthesis tedious and prone to difficulties with solubility and reactivity of the precursors, which would themselves have rather extended π-systems. Furthermore, there exists the possibility that a Peierl's distortion would occur for such a large π-system as, for example, that which occurs in polyacetylene and is predicted for polyacene,[6] thereby counteracting the effect of enlarging the π-system. Nonalternant systems therefore seemed more attractive candidates. While cyclohepta[*def*]fluorene and the cyclohepta[*a*]cyclopenta[*i*]anthracene systems have low HOMO−LUMO splittings, examination of the AO coefficients of the frontier orbitals indicates little spatial overlap, similarly to those of azulene, of which these compounds are derivatives. This suggests a small exchange interaction ($K_{HO,LU}$) and therefore little preference for the promotion of an electron to the LUMO, as required for a triplet ground state. Azulene has a very small S_1-T_1 energy of 7 kJ mol^{-1},[13] indicative of the small exchange interaction between the frontier orbitals. An isoelectronic heteroanalogue of cyclohepta[*def*]fluorene was found to have a singlet ground state.[14]

The HOMO−LUMO gap of 2,2-dimethyl-2*H*-benzo[*cd*]-fluoranthene (**1**) is 0.17β at the Hückel level, and the spatial overlap of these frontier orbital indicates a large exchange interaction ($K_{HO,LU}$). The close structural relationship between **1** and known 1,8-naphthoquinodimethanes[15,16] suggested the synthetic route to the photoprecursors.

† Present address: Merck & Co, Inc., Molecular Systems, WP53F-301, P.O. Box 4, West Point, PA 19486.

(1) Longuet-Higgins, H. C. *J. Chem. Phys.* **1950**, *18*, 265−274.
(2) Hoffmann, R. *J. Am. Chem. Soc.* **1968**, *90*, 1475.
(3) Baumgartner, P.; Weltin, E.; Wagnière, G.; Heilbronner, E. *Helv. Chim. Acta* **1965**, *48*, 751−764.
(4) Gleicher, G. J.; Newkirk, D. D.; Arnold, J. C. *J. Am. Chem. Soc.* **1973**, *95*, 2526−2531.
(5) Angliker, H.; Rommel, E.; Wirz, J. *Chem. Phys. Lett.* **1982**, *87*, 208−212.
(6) Roncali, J. *Chem. Rev.* **1997**, *97*, 173−205.
(7) Aihara, J. *Bull. Chem. Soc. Jpn.* **1975**, *48*, 3637−3640.
(8) Hochmann, P.; Zahradnik, R.; Kvasnicka, V. *Collect. Czech. Chem. Commun.* **1968**, *33*, 3478−3513.
(9) Kolc, J.; Michl, J. *J. Am. Chem. Soc.* **1970**, *92*, 4147−4148.
(10) Michl, J.; Kolc, J. *J. Am. Chem. Soc.* **1970**, *92*, 4148−4150.
(11) Steiner, R. P.; Michl, J. *J. Am. Chem. Soc.* **1978**, *100*, 6413−6415.
(12) Castellan, A.; Kolc, J.; Michl, J. *J. Am. Chem. Soc.* **1978**, *100*, 6687−6692.
(13) Murov, S. L.; Carmichael, I.; Hug, G. L. *Handbook of Photochemistry*, 2nd ed.; Marcel Dekker: New York, 1993; p 420.
(14) Freiermuth, B.; Wirz, J. *Angew. Chem., Int. Ed. Engl.* **1988**, *27*, 585−587.

10.1021/ja0004377 CCC: $20.00 © 2001 American Chemical Society
Published on Web 12/16/2000

Scheme 1: Photochemical Generation of **1** and **2**

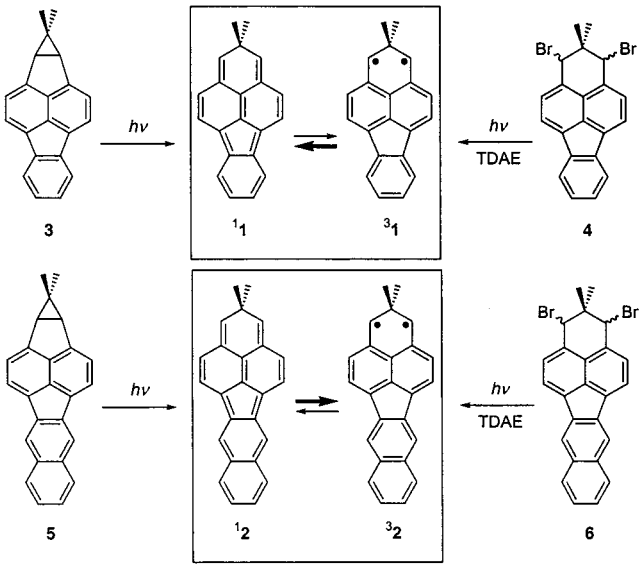

We present the synthesis and spectroscopy of two Kekulé diradicals, 2,2-dimethyl-2*H*-benzo[*cd*]fluoranthene (**1**) and 2,2-dimethyl-2*H*-dibenzo[*cd*,*k*]fluoranthene (**2**).[17] We report the details of the synthesis and low-temperature matrix spectroscopy of **1** and **2** and give the results of experiments on the room-temperature solution chemistry of these compounds and calculations. These experiments allow an estimation of the singlet−triplet splitting of the two compounds. While **1** is a ground-state singlet, displaying the long-wavelength electronic absorption characteristic of an extended quinonoidal π-system and no EPR spectrum, **2** is a triplet in the ground state, with a UV−vis spectrum similar to that of known 1,8-naphthoquinodimethane derivatives and an EPR spectrum characteristic for a triplet-state molecule.

Results

Synthesis. Compounds **1** and **2** were generated from two separate photoprecursors each, the cyclopropanes **3** and **5** and the dibromides **4** and **6**, as shown in Scheme 1. The synthesis of **3**−**6** entailed conventional organic chemistry; therefore, only those aspects relevant to the spectroscopic studies presented in the next section are described here. The experimental details of the synthesis are available as Supporting Information.

The synthetic route, presented in Scheme 2, was based on the work of Hasler et al.[15] The greatest difficulty was encountered in the conversion of dibromide **4** to cyclopropane **3**. Whereas Hasler's naphthalene analogue of **4** can be converted to the cyclopropane using lithium amalgam in degassed benzene in acceptable yield, **4** gave only the reduced compound **9** under identical conditions. After considerable experimentation, Zn dust in DMF was found to yield the desired cyclopropane **3** in moderate yield. The reaction also yields the reduced compound **9**, which could not be removed chromatographically.

Cyclopropane **3** is thermally stable at room temperature but reacts with oxygen to give keto aldehyde **10** when allowed to stand in aerated solution. The formation of **10** presumably occurs by interception of **1** by oxygen to form endoperoxide **11**, which reacts further to yield the stable **10** (Scheme 3). Autoxidation was observed previously by Hasler et al. for a bis(cyclopropane)-naphthalene.[16] The reaction of O_2 with **1** was examined by ns flash photolysis (vide infra). The cyclopropane **3** decomposes to **10** in the presence of air at room temperature with a lifetime on the order of a few days. This is in stark contrast to Hasler's naphthalene analogue, which is stable in the presence of air for months, and to a bis(cyclopropane) analogue, which was converted to the corresponding keto aldehyde after 2 days under 50 atm of oxygen.[16] Thoroughly degassed solutions of **3** did not show any appreciable decomposition over the course of several days; nevertheless, most experiments were performed using freshly prepared **3**.

Similarly to the reaction of **4** to **3**, formation of **5** is accompanied by formation of the reduced compound, albeit to a lesser extent. Whereas **3** generally contains 30−70% **9**, **5** has been synthesized with only approximately 10% reduced compound. Cyclopropane **5**, like **3**, undergoes reaction with O_2, forming the analogous keto aldehyde. While **3** decomposed in air within a few days, **5** is even more air-sensitive, reacting with a lifetime of around 1 day.

Electronic Absorption Spectra of 1. Irradiation of cyclopropane **3** in a rigid, degassed 2-methyltetrahydrofuran (MTHF) matrix at ~81 K with 365-nm light causes the appearance of several absorption bands in the UV, visible, and near-IR regions. All of the bands grow in at the same rate and disappear irreversibly upon warming the matrix. Figure 1 displays the difference spectra obtained at two different concentrations. No correction was made for bleaching of **3** below 410 nm.

Irradiation at 365 nm causes extensive conversion of **3** within a few minutes, after which the reaction slows down. Prolonged irradiation at 365 nm or with the unfiltered Hg arc output leads to further slow growth. The photoproduct therefore acts as a filter: it absorbs strongly in the UV, especially at 365 nm, thereby decreasing the amount of light available to **3**. The product is photostable: irradiation with either the unfiltered output of an arc lamp or using a Schott GG455 long-pass filter causes no decrease in the new spectral features. Irradiation with the GG455 filter in place (λ > 455 nm) also tests for a photochemical equilibrium between **3** and the photoproduct. That no loss of photoproduct is observed indicates that the product cannot be reverted to **3** photochemically at a measurable rate.

The same spectral features are obtained by irradiation of cyclopropane **3** in polyethylene and by irradiation of a dibutyl phthalate matrix containing 0.03 M dibromide **4** and 0.1 M tetrakis(dimethylamino)ethylene (TDAE), which renders the matrix opaque below 500 nm. The band at 528 nm imparts a reddish to orange-reddish color to the matrix; this characteristic color is also observed upon irradiation of **3** in a variety of other matrices: 3-methylpentane, methylcyclohexane, CH_2Cl_2, adamantane, phenyl salicylate, and poly(methyl methacrylate). On the basis of the methods of generation and agreement with the spectrum calculated by PPP-SDCI,[17] this spectrum is assigned to 2,2-dimethyl-2*H*-benzo[*cd*]fluoranthene (**1**).

Bands 1, 3, and 4 display vibrational progressions with a separation of 1300−1500 cm^{-1}, typical for polycyclic unsaturated hydrocarbons; a shoulder at approximately 680 nm and a weak peak at 620 nm may be due to a vibrational progression in band 2, likewise of ~1400 cm^{-1} separation. When **1** is generated from **3** in an MTHF glass, isosbestic points are observed at 390 and 403 nm. The molar absorption coefficients were estimated on the basis of the assumption that the intensities of the strong bands of cyclopropane-fused fluoranthene **3** are

(15) Hasler, E.; Gassmann, E.; Wirz, J. *Helv. Chim. Acta* **1985**, *68*, 777−788.

(16) Hasler, E.; Hörmann, A.; Persy, G.; Platsch, H.; Wirz, J. *J. Am. Chem. Soc.* **1993**, *115*, 5400−5409.

(17) McMasters, D. R.; Wirz, J.; Snyder, G. J. *J. Am. Chem. Soc.* **1997**, *119*, 8568−8569.

Scheme 2: Synthesis of Photoprecursors to **1**

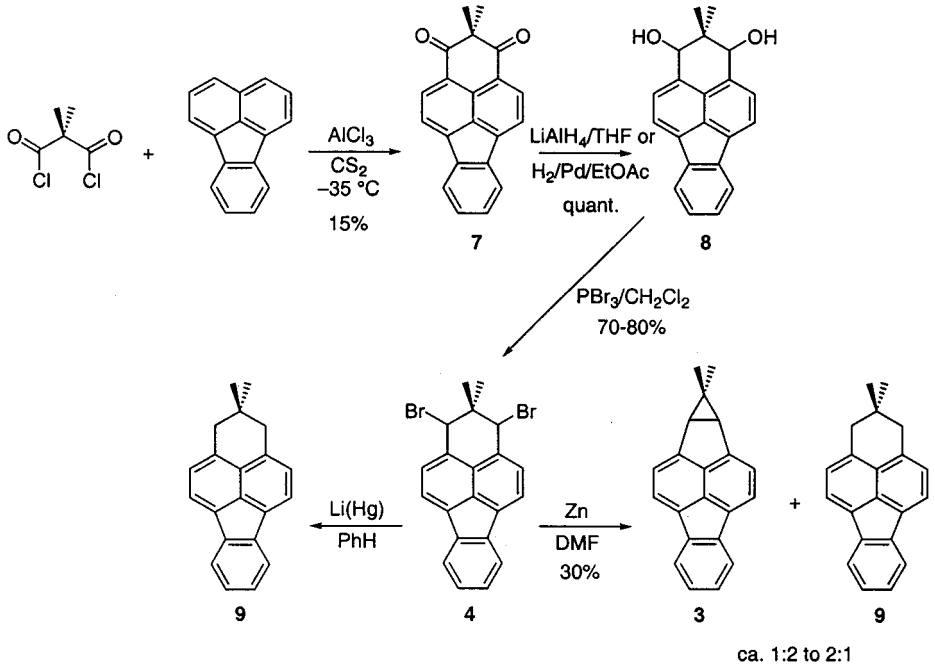

Scheme 3: Reaction of **3** with O_2

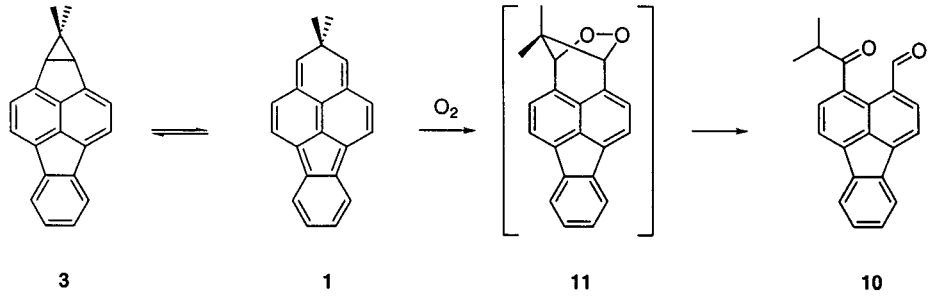

essentially the same as those of fluoranthene itself. The absorption of the new bands could then be related to the absorption of the starting material at 370 nm, assuming clean conversion, or to the loss of absorption at 300 nm, assuming that the photoproduct has no sharp features in this region. For bands 1 and 2, this gave log $\epsilon \approx 3.0$, for band 3, log $\epsilon \approx 3.9$, and for band 4, log $\epsilon \approx 4.7$.

As previously reported,[17] the observed spectrum of **1** is poorly reproduced by both Pariser−Pople−Parr−Mataga (PPPM) singlet and triplet calculations. While the calculation predicts an S_0-S_1 transition in the near-IR, which is of almost pure HOMO−LUMO character, the transitions observed at higher energy are very poorly reproduced. The calculated triplet spectrum shows even less agreement. We obtained decent agreement with PPP-SDCI calculations, in which doubly excited configurations are included in the configuration matrix. These calculations show excellent agreement with the experiment for the S_0-S_1 and S_0-S_2 transitions, but are unable to reproduce the higher-energy transitions accurately.

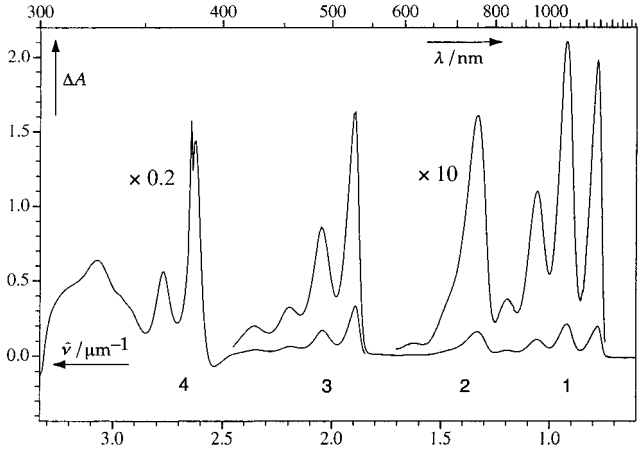

Figure 1. Difference spectrum of **1** generated by 365-nm irradiation of cyclopropane **3** in MTHF glass at ~81 K.

To gain more information regarding the electronic structure of **1**, as well as to assist the assignment of the calculated transitions to the observed bands, the transition moment directions were measured using oriented samples of **1** in stretched polyethylene.[18] The results, presented in Figure 2, were obtained at two separate concentrations. The *z*-direction orientation factor obtained was $K_z = 0.6$, comparable to similarly shaped polycyclic aromatic hydrocarbons. The spectra are reducible into a parallel (*z*-) component, which contains bands 2, 3, and 4, and a perpendicular (*y*-) component, with peaks at 1310, 1100, and 950 nm, all belonging to the S_0-S_1 band, but featureless below 800 nm down to 400 nm. The step at 860 nm is due to a baseline shift where the detector changes; above 860 nm, the PbS detector was used, leading to more noise at the relatively high sensitivity level used.

(18) Michl, J.; Thulstrup, E. W. *Spectroscopy with Polarized Light*; VCH Publishers: New York, 1986, 573 pp.

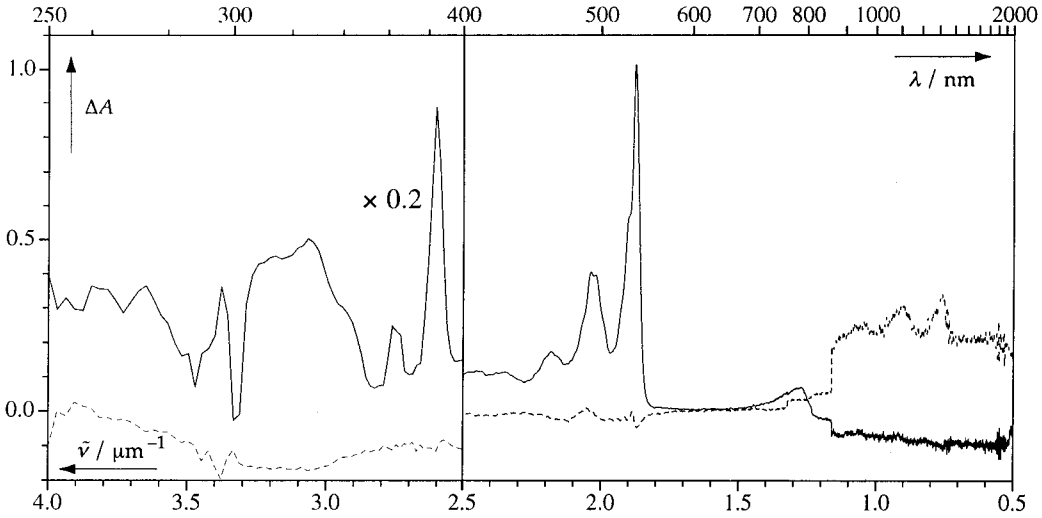

Figure 2. Reduced polarized spectra of **1** in stretched polyethylene: E_z (long-axis polarized), solid; E_y (short in-plane axis polarized), dashed.

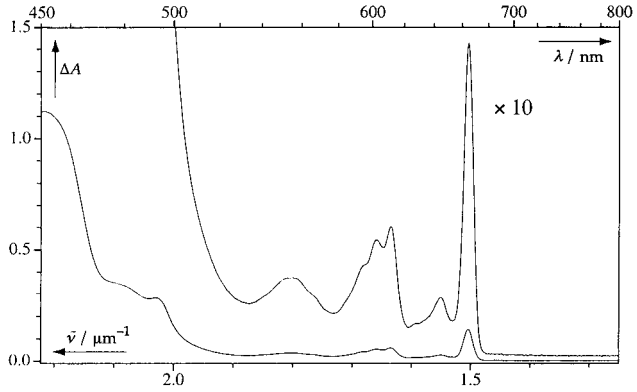

Figure 3. UV−vis spectrum of **2**.

Electronic Absorption Spectrum of 2. Irradiation of cyclopropane **5** in an MTHF glass at 81 K with 405-nm light gives rise to a series of new peaks in the visible region, as well as changes in the ultraviolet, which are persistent under these conditions (Figure 3). The newly formed species is photostable, withstanding the unfiltered, focused output of a 200-W Hg arc lamp, as well as the output filtered with a Schott OG530 long-pass filter ($\lambda > 530$ nm) (to exclude the possibility of a photochemical equilibrium between **2** and either cyclopropane **5** or another species), but quickly decays on thawing the matrix. The spectrum is characterized by a relatively weak ($\epsilon \approx 900$), extremely narrow peak at 665 nm, followed by weaker peaks at 610 and 555 nm, then stronger absorption below 500 nm. A very strong peak ($\epsilon \approx 60\,000$) appears at 343 nm. No new absorptions were observed beyond 665 nm out to 2200 nm, beyond which wavelength MTHF is opaque.

The peak at 665 nm, with a full width at half-maximum (fwhm) of approximately 190 cm^{-1}, is significantly narrower than the 0−0 transitions of **1**, which have fwhm's of around 600 cm^{-1} (with the exception of the 750-nm transition, which is broader still). The narrowness of this transition indicates that both the ground and first excited electronic states of **2** have well-defined minima. Furthermore, such narrow bands in the absorption spectrum have often been observed for ground-state triplets[16,19] and may be considered diagnostic for triplet species.[20] The first absorption band shows a complex vibrational pattern, with major progressions of about 1300 cm^{-1}, and minor progression of ~450 and 250 cm^{-1} discernible in the first and second major group of vibronic bands, respectively. The third major group is not vibrationally resolved. Isosbestic points were observed at 423, 409, 400, 386, 326, 285, 283, 278, and 276 nm.

Analogously to the generation of **1** from dibromide **4** by irradiation in a matrix containing TDAE, **2** should be accessible by irradiation of dibromide **6** under the same conditions. Because of the difficulty of separation, a mixture of isomeric dibromides **6** and **12** (Scheme 4) was used. Irradiation of a frozen solution of MTHF containing 0.03 M of an approximately 1:1 mixture of dibromides **6** and **12** as well as approximately 0.1 M TDAE caused the formation of new spectral features throughout the visible region of the spectrum. Most of these spectral features are assigned to **13**, which is predicted by PPPM calculations to have a strong transition in the visible at 563 nm. The weaker transitions of **2** are mostly buried underneath the absorptions of **13**. However, the sharp peak seen at 665 nm and attributed to **2** was observed overlying the spectrum of **13**.

Scheme 4

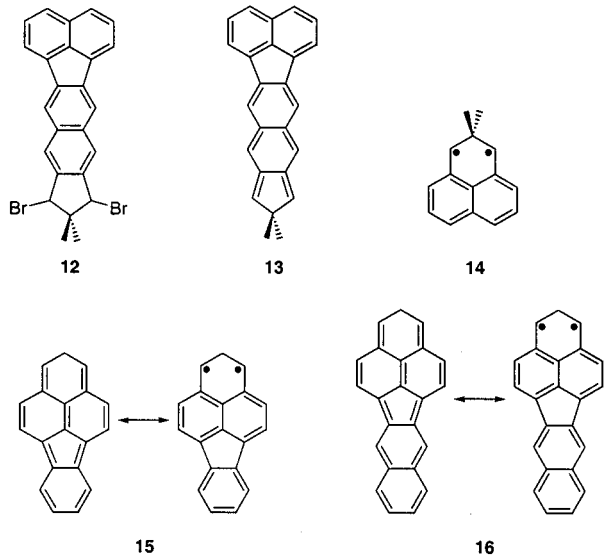

The calculated spectrum of singlet **2** using PPPM calculations either with or without doubly excited configurations shows much longer wavelength absorptions than are observed experimentally. The PPP-SDCI calculation predicts moderately strong bands at

(19) Gisin, M.; Rommel, E.; Wirz, J.; Burnett, M. N.; Pagni, R. M. *J. Am. Chem. Soc.* **1979**, *101*, 2216−2218.

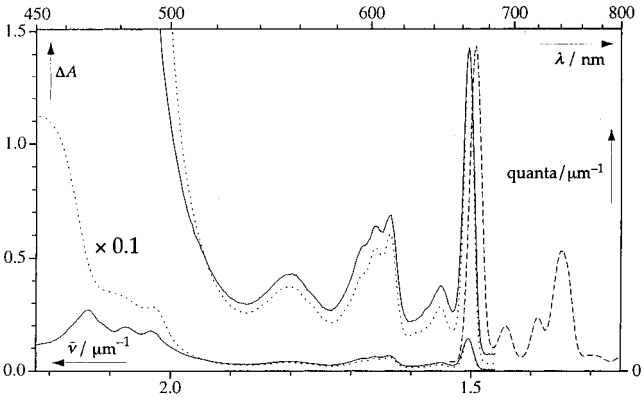

Figure 4. Excitation (λ_{em} = 740 nm; solid line) and emission (λ_{ex} = 466 nm; dashed) spectra of **2** in MTHF glass at 77 K, along with the absorption spectrum of Figure 3 (dotted). Emission spectrum is corrected.

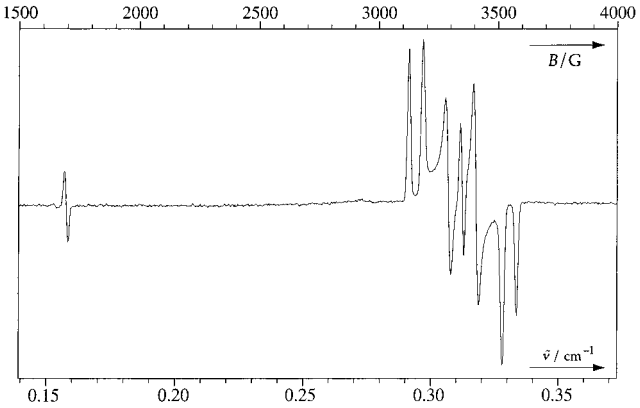

Figure 5. EPR spectrum of **2** generated by 405-nm irradiation (5 min. of irradiation with a 1000-W Hg(Xe) arc lamp filtered by UG5 and 405-nm band-pass filters) of cyclopropane **5** in MTHF glass at 90 K. Microwave power = 2 mW.

1338 and 759 nm. Modest agreement with experiment is obtained using triplet-state PPP calculations,[21] which predict the longest-wavelength transition at 604 nm.

Irradiation of **5** in a rigid dibutyl phthalate matrix at temperatures between 120 and 150 K causes the growth of spectral features essentially identical to those depicted in Figure 3. At these temperatures, the signal shows relatively rapid decay which can be conveniently followed at 665 nm. While the 130 K decay curve fits a monoexponential function relatively well, with a lifetime of approximately 1 h ($k = 2.9 \times 10^{-4}$ s^{-1}), the other decay curves show more complex kinetics. This is typical for reactions in matrices, and may be attributed to the presence of various nonequivalent sites in the matrix, each with a different kinetic behavior.

Irradiation of diradical **2** in glassy matrices gives rise to a red fluorescence emission. Figure 4 depicts the excitation and emission spectra obtained in the range of 450−800 nm. They are independent of the wavelength of observation and excitation, respectively: emission spectra obtained by exciting at 466 and 610 nm are essentially identical, as are excitation spectra obtained by observing at 670 and 740 nm. The absorption and excitation spectra are in excellent agreement down to around 460 nm, below which point unconverted **9** and keto aldehyde begin absorbing. Emission peaks are also observed at 803 and 826 nm. The emission shows a major vibrational mode of 1410 cm^{-1} and minor mode of about 500 cm^{-1}, compared with 1300 and 450 cm^{-1} in the absorption. The vibrational structure of the emission spectrum is similar to that of benzo[*k*]fluoranthene itself, which displays fluorescence emission between 400 and 500 nm with vibrational modes of 1490 and 550 cm^{-1} (1450 and 550 cm^{-1} in the absorption spectrum). The fluorescence of **2** was also observed upon irradiation with an excimer laser with a pulse width of ∼25 ns. The decay of the fluorescence followed the temporal profile of the laser pulse; thus, the fluorescence has a lifetime of 25 ns or less.

EPR Spectroscopy of 1. No triplet EPR signal was observed after irradiation of **3** in a degassed MTHF matrix at 89 K, which displayed the red, persistent color characteristic of **1**. Weak, wide triplet signals ($|D/hc|$ = 0.0751 cm^{-1}, $|E/hc|$ = 0.0043 cm^{-1}) observed *during* the irradiation were found in a control experiment to be due to triplet excited **9**. Experiments involving TDAE and either the dibromide **4** or the analogous dichloride gave only doublet signals.

Attempts to detect thermal population of the triplet state ^{3}**1** at higher temperatures also failed to give a perceptible triplet signal. To thermally populate the triplet state as much as possible, matrix materials with higher glass transition temperatures than MTHF were used, namely dibutyl phthalate, phenyl salicylate, and poly(methyl methacrylate), which have T_g values of ∼180, 200, and 370 K, respectively. It was found that the orange-red color of ^{1}**1** persists up to 170 K in all three of these matrix materials and up to nearly 200 K in the latter two. Red samples of **1** in these matrices gave no discernible triplet EPR signals at temperatures up to 170 K. To determine a minimum singlet−triplet gap from this observation, the sensitivity of the EPR spectrometer and the concentration of **1** in the sample are needed, both of which data are not known accurately. However, on the basis of the observed signal-to-noise ratio in the EPR spectrum of ^{3}**2** (Figure 5) and assuming the same sensitivity and concentration, a minimum value of $E_T - E_S$ = 1.2 kcal mol^{-1} is estimated. In fact, during the many attempts, the instrumental settings were adjusted and many spectra were accumulated, so that the sensitivity was probably much higher. Lacking knowledge of the exact concentration of **1**, however, we can only state with confidence that $E_T - E_S \geq 1$ kcal mol^{-1}.

EPR Spectroscopy of 2. Irradiation of cyclopropane **5** in an MTHF glass at ∼90 K with 405-nm light in the cavity of an EPR spectrometer gives rise to the spectrum reproduced as Figure 5, characteristic of a randomly oriented triplet; this spectrum is persistent and stable at 90 K in the dark. Thawing the MTHF glass causes the irreversible destruction of the carrier of the triplet signal; re-irradiating the refrozen, EPR-silent glass leads once again to the spectral features of Figure 5. The same spectral features are obtained by irradiation of dibromides **6** and **12** in a glassy matrix of MTHF or methylcyclohexane containing TDAE; in this case, however, the central two Δm_s = 1 lines are obscured by a strong monoradical impurity. Analysis of the spectra yields the zero-field splitting parameters $|D/hc|$ = 0.0210 cm^{-1} and $|E/hc|$ = 0.0034 cm^{-1}. On the basis of the *D*-value and the methods of generation, these spectra are assigned to triplet **2**. The *D*-value is slightly smaller than that of **14** ($|D/hc|$ = 0.029 cm^{-1}), consistent with delocalization of spin through the larger π-system. No fine structure is observed for any of the EPR transitions at either 6 or 90 K, and down to a modulation amplitude of 0.1 G.

The spectrum in Figure 5 is virtually free of paramagnetic impurities. The central peak at 3340 G is due primarily to a double quantum transition, as demonstrated by its overproportional dependency on the microwave power: decreasing the microwave power to 20 μW caused the central peak to almost disappear.

Generation of **2** in dibutyl phthalate glass in the EPR cavity

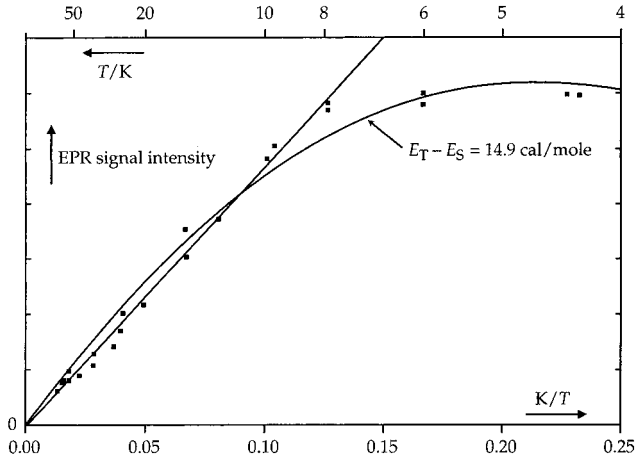

Figure 6. Curie plot of **2**. The straight line is a least-squares fit to the data, excluding the four points obtained at 6 and 4 K. The curved line represents the fit of all data points to the equation for a thermally excited triplet state.

held at 120 to 140 K gives rise to its characteristic triplet spectrum such as depicted in Figure 5, which slowly diminishes in intensity at a rate on the same order as that observed by UV−vis spectroscopy between 120 and 150 K.

The temperature dependence of the EPR signal intensity of ^{3}**2** is presented in Figure 6. The signal intensity I refers to the integrated area of the two outermost peaks of the $\Delta m_s = 1$ manifold. The straight line represents a least-squares fit of the points above 6 K to the equation: $I = aT + b$. The intercept b is zero in the Curie law. Although b was not forced to equal zero, the best fit passed very near the origin.

The data reveal a linear behavior between 8 and 75 K. Plotting the double integral of the $\Delta m_s = 2$ peak against $1/T$ also gives linear behavior in the range of 8−75 K. Deviation from linearity below 8 K is presumably caused by signal saturation, errors in temperature measurement, or both; such deviations at extremely low temperature have been seen for other ground-state triplets.[19] A linear Curie plot is also consistent with very nearly degenerate lowest singlet and triplet states. To determine the maximum singlet−triplet gap consistent with the observed data, the data were fitted to the modified form of the Curie law valid for triplet states in equilibrium with a singlet state:[22]

$$I = \frac{C}{T} \cdot \frac{3e^{-\Delta E/RT}}{1 + 3e^{-\Delta E/RT}}$$

where I represents the signal intensity, C a constant, and ΔE the singlet−triplet splitting. The fit was relatively poor and yielded the parameter $\Delta E = +0.015$ kcal mol^{-1}, that is, a singlet ground state with the triplet state lying 15 cal mol^{-1} higher in energy. Thus, the Curie data for **2** are consistent with either a triplet ground state or a thermally populated triplet state lying no more than 0.02 kcal mol^{-1} above the singlet ground state.

Flash Photolysis and Trapping. Irradiation of degassed acetonitrile solutions of **3** with laser pulses of ∼25 ns duration and 248 or 351 nm wavelength gave rise to a transient of several-millisecond lifetime, which was followed kinetically at 380 and at 528 nm. At low laser power, the decay of the signal shows satisfactorily first-order kinetics with a lifetime of 6 ms. Spectrographic flash photolysis 900 μs after the laser pulse provided the difference spectrum of this transient, which is depicted in Figure 7 overlaid with the difference spectrum obtained by irradiation of **3** in MTHF glass at 81 K (Figure 1). The transient species is assigned as ^{1}**1**.

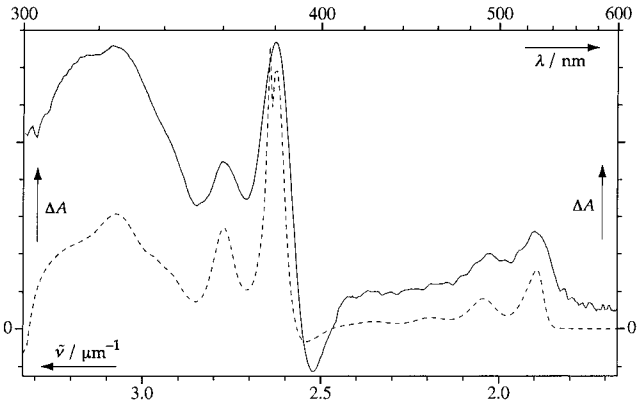

Figure 7. Difference spectrum of ^{1}**1**: in MTHF glass at 81 K (dotted) and in acetonitrile at room temperature (solid).

Table 1: Estimated Rate Constants of Trapping of **1** with Olefins

	τ	k/M^{-1} s^{-1}
1 M AN	3 ms	$<3 \times 10^2$
0.1 M MA	800 ms	1.3×10^4
1×10^{-4} M MTAD	25 ms	4×10^8
1×10^{-4} M TCNE	5 ms	2×10^9

Saturation of the CH_3CN solution with air shortens the lifetime of **1** to 19 μs, while in O_2-saturated solution, the lifetime was 3.8 μs. The concentration of O_2 in air-equilibrated CH_3CN has been measured as 2.42 mM;[23] a lifetime of 19 μs therefore indicates an estimated second-order reaction rate constant of 2.2×10^7 M^{-1} s^{-1}. This value is 3 orders of magnitude slower than the bimolecular diffusion-controlled limit of $\sim 2 \times 10^{10}$ M^{-1} s^{-1}.

Several dienophiles were examined as traps for **1**: acrylonitrile (AN), maleic anhydride (MA), tetracyanoethylene (TCNE), and 4-methyl-1,2,4-triazoline-3,5-dione (MTAD). The rate constants estimated from the observed lifetimes τ in the presence of these reactants are presented in Table 1. While AN reacted sluggishly if at all, more reactive dienophiles trapped **1** effectively, TCNE at a rate approaching the diffusion-controlled limit. The product of reaction between **1** and TCNE was isolated (see Supporting Information).

Irradiation of a degassed acetonitrile solution of cyclopropane **5** with a 248-nm laser pulse (25 ns pulse width) results in the formation of a strong transient absorption at 343 nm within the laser pulse width. The decay of this signal obeys first-order kinetics with a lifetime of 57 μs. Spectrographic detection at a delay of 100 ns after the laser pulse provided the difference spectrum. Figure 8 shows this transient difference spectrum, overlaid with the difference spectrum obtained by irradiation of **5** in MTHF glass at 81 K. The transient species is assigned as ^{3}**2**. The primary photoproduct upon irradiation of **5** is presumably ^{1}**2**. No other transient absorptions were observed prior to those assigned to ^{3}**2**, indicating that intersystem crossing is complete within around 25 ns: k_{ISC} (^{1}**2** → ^{3}**2**) > 4×10^7 s^{-1}.

The lifetime of **2** in aerated CH_3CN is 1.1 μs, while saturation with pure oxygen shortens the lifetime to ∼400 ns. The latter

(20) Diradicaloid species usually have a lowest singlet state that lies in a shallow potential energy minimum with respect to at least one reaction coordinate (e.g., cyclopropane ring closure in the case of compounds **1** and **2**), and electronic transitions from that state are commonly diffuse. In contrast, the lowest triplet state of the same species is strongly bound, because the same reaction(s) on the triplet surface leads to an excited triplet state of a closed-shell species.

(21) Gisin, M.; Wirz, J. *Helv. Chim. Acta* **1983**, *66*, 1556−1568.

(22) Breslow, R.; Chang, H. W.; Hill, R.; Wasserman, E. *J. Am. Chem. Soc.* **1967**, *89*, 1112−1119.

(23) Franco, C.; Olmsted, J., III. *Talanta* **1990**, *37*, 905−909.

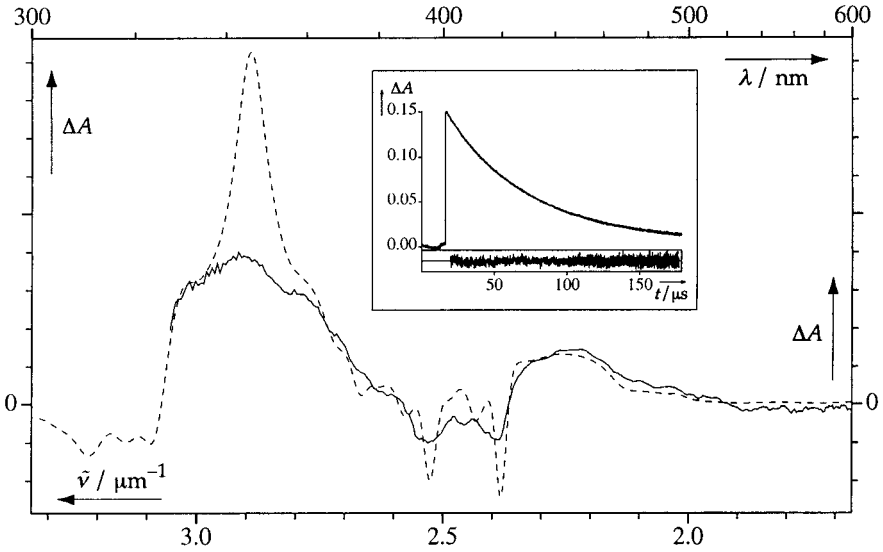

Figure 8. Difference spectrum of ^{3}**2**: in MTHF glass at 81 K (dotted) and in acetonitrile at room temperature (solid). The inset shows the decay of absorbance at 343 nm.

measurement was hindered by the reaction of **5** with oxygen even prior to laser irradiation. On the basis of the measurement with aerated CH_3CN, the second-order rate constant for reaction of **2** with O_2 is estimated at 5×10^8 M^{-1} s^{-1}. This value is roughly 1 order of magnitude less than the diffusion-controlled limit ($\sim 2 \times 10^{10}$ M^{-1} s^{-1}). Due to spin statistics, only one in nine complexes between two triplet-state molecules has singlet multiplicity. Taking this into account, the reaction of **2** with oxygen approaches the diffusion-controlled limit. The lifetime of **2** in degassed CH_3CN was not changed by addition of 1 M acrylonitrile. Therefore, the second-order rate constant for reaction with acrylonitrile is less than 10^4 M^{-1} s^{-1}.

Calculations. Density functional theory calculations were performed on the lowest singlet and triplet states of compounds **15** and **16**, relatives of **1** and **2**, respectively, in which the methyl groups have been replaced by H atoms for the sake of computational feasibility. The calculations were performed at the B3LYP/6-31G* level and included full geometry optimization at the same level of theory.

It has been suggested that the use of UHF wave functions to calculate the singlet state leads to an error known as spin contamination.[24] The UHF singlet energy contains some triplet wave function admixture which biases the calculated singlet energy toward that of the triplet, decreasing the absolute singlet−triplet gap. The spin contamination can be removed with the aid of the parameter $\langle S^2 \rangle$, which is a measure of the radical character (the unpaired spin) of the calculated singlet wave function, in a procedure known as spin projection.[24−26] For the pure (nonspin-contaminated) singlet wave function, $\langle S^2 \rangle$ should equal 0, while $\langle S^2 \rangle = 2$ for the triplet.

The results of the B3LYP/6-31G* calculations are shown in Table 2. **15** is predicted to be a ground-state singlet, while **16** is calculated to have a triplet ground state. This is true for both the spin-contaminated and spin-corrected energies. The prediction of a singlet ground state for **15**, the nonmethylated analogue of **1**, and a triplet ground state for **16**, the analogue of **2**, is in gratifying agreement with the experimental results on **1** and **2**.

Table 2: Results of Density Functional Theory Calculations, in kcal mol^{-1}

	15	**16**	$\Delta\Delta E_{ST}$
$E_T - E_S$ (spin-contaminated)	0.7	−1.3	2.0
$E_T - E_S$ (spin-corrected)	1.2	−2.4	3.6

The geometries calculated for the electronic ground states, ^{1}**1** and ^{3}**2**, are very similar, displaying little bond alteration, indicating that the singlet state, too, has significant diradical character.

Besides the individual singlet−triplet gaps ΔE_{ST}, the difference in singlet−triplet gap for the two compounds, $\Delta\Delta E_{ST}$, is an important value, which can be derived from the calculations. While the singlet−triplet gap predicted by the calculations may be off by several kcal mol^{-1} for a given compound, the error may expected to be similar for compounds **1** and **2**, in which case $\Delta\Delta E_{ST}$ should be more accurate. Furthermore, the fact that the methyl groups of **1** and **2** were neglected in the calculation will cause a systematic deviation between the experimental results and the calculation, which however should be substantially compensated for in the case of $\Delta\Delta E_{ST}$.

Discussion

The exchange interaction between two electrons in the HOMO and LUMO, $K_{HO,LU}$, determines not only the amount of stabilization of the triplet state, $\Delta E(S_1-T_1)$, but is also the off-diagonal element responsible for mixing of the ground configuration (χ_0) with the doubly excited configuration $\chi_{1,1}^{-1,-1}$. Consequently, the relatively large value of $K_{HO,LU}$ (**1**) is expected to manifest itself not only in a low-lying triplet state, but also in a substantial contribution of $\chi_{1,1}^{-1,-1}$ to low-lying electronic states.[27]

The excellent agreement between the experimental spectrum and the calculated spectrum using the PPP-SDCl program clearly demonstrates that the transition at 750 nm is to an excited state which is of largely doubly excited, $\chi_{1,1}^{-1,-1}$, character. The configuration $\chi_{1,1}^{-1,-1}$ contributes around 50% to this state according to the calculation, while the ground configuration χ_0 accounts for 10%, and the $1'(-2)$ and $2'(-1)$ singly excited configurations provide around 20% each.

(24) Yamaguchi, K.; Jensen, F.; Dorigo, A.; Houk, K. N. *Chem. Phys. Lett.* **1988**, *149*, 537.
(25) Yamanaka, S.; Kawakami, T.; Nagao, H.; Yamaguchi, K. *Chem. Phys. Lett.* **1994**, *231*, 25−33.
(26) Goldstein, E.; Beno, B.; Houk, K. N. *J. Am. Chem. Soc.* **1996**, *118*, 6036−6043.
(27) Leupin, W.; Wirz, J. *J. Am. Chem. Soc.* **1980**, *102*, 6068−6075.

The first reported observation of a state of predominantly doubly excited character was for pleiadene.[28] The second band appeared as a weak, long-wavelength shoulder on the strong third band and was assigned as a doubly excited-state based on PPP-SDCI calculations. In contrast to pleiadene, **1** shows a very strong transition to a doubly excited state, which is well separated from transitions due to higher-lying configurations. In fact, **1** represents perhaps the best example to date of such a state isolated from higher transitions. The fact that the transition to a doubly excited state in **1** is so well resolved from transitions involving higher-lying configurations is a consequence of the small HOMO−LUMO gap of **1** and the magnitude of $K_{HO,LU}$. This is also evident from the substantial admixture, 10%, of $\chi_{1,1}^{-1,-1}$ in the ground state.

A direct experimental determination of the singlet−triplet splitting of **2** is contingent upon observation of a thermal Boltzmann population of the lowest singlet state. EPR is unsuitable in this regard: the singlet state is EPR-silent, and, as has been discussed elsewhere,[29,30] Curie plots are extremely insensitive to low-lying excited singlet states.

The observation of a linear Curie plot for ^{3}**2** demonstrates that the triplet state is either the ground state or very nearly degenerate with the singlet ground state, that is, within 0.02 kcal mol^{-1} of it. Such an accidental degeneracy can be discounted on the basis of the UV−vis/NIR data, however. In the case of degeneracy, the singlet would make up 25% of the sample population (the triplet makes up 75% because it is 3-fold degenerate, each of its three sublevels contributing 25%). The S_0-S_1 transition of **2** is calculated by the PPP-SDCl program to have a molar absorption coefficient $\epsilon = 1500$ ($\lambda = 1338$ nm), and the S_0-S_2 transition $\epsilon = 5400$ ($\lambda = 759$ nm). The analogous transitions were calculated satisfactorily for **1**, both in terms of position, polarization and intensity, which was within a factor of about 2 of the experimental estimate for both transitions. Were ^{1}**2** present in one-third the concentration of ^{3}**2**, the S_0-S_1 and S_0-S_2 absorbances would be approximately as intense as the observed T_0-T_1 peak at 665 nm. No absorbances assignable to ^{1}**2** were discernible out to 2200 nm, however, above which wavelength MTHF is opaque. The absence of bands corresponding to either the S_0-S_1 or the S_0-S_2 transition (Figure 3) is untenable with degenerate singlet and triplet states. In fact, these bands would also be observable in the case of a thermally populated excited singlet state. The absence can be used to estimate the minimum singlet−triplet gap for **2**. Combining the observed signal-to-noise ratio, the molar absorption coefficient of the triplet state, the calculated molar absorption coefficient for the singlet state, and the statistical preference for the (3-fold-degenerate) triplet state, a minimum singlet−triplet splitting of 0.8 kcal mol^{-1} is estimated.

Like many triplet compounds, ^{3}**2** reacts with oxygen at nearly the (spin-statistically corrected) diffusion-controlled limit. If we assume that ^{3}**1** also reacts with oxygen at this rate, we can use the observed rate of reaction of photochemically generated **1** with oxygen to calculate the amount of **1** present in the triplet state. Further assuming that intersystem crossing from ^{1}**1** to ^{3}**1** is fast relative to the observed decay, which seems likely given the fast intersystem crossing of **2** (k_{ISC} (^{1}**2** → ^{3}**2**) > 4×10^7 s^{-1}, at least 3 orders of magnitude faster than the observed reaction of **1** with O_2), this allows us to estimate the singlet−triplet gap for **1**. Since $[k(O_2)(\mathbf{2})/k(O_2)(\mathbf{1})] = 16$, ($[^3\mathbf{1}]/[^1\mathbf{1}]$) = 0.06. Using $\Delta E \approx -RT \ln K$ and including the statistical preference for the triplet state, we conclude that the singlet−triplet gap for **1** is about 2.3 kcal mol^{-1}.

An upper limit for ΔE_{ST} can be estimated on the basis of the estimate of the singlet−triplet gap of **1** along with the results of density functional calculations. According to the calculations, the difference in ΔE_{ST} between **1** and **2** does not exceed 3.6 kcal mol^{-1}. Given our prediction that $E_T - E_S$ (**1**) ≈ 2.3 kcal mol^{-1}, we expect that $E_T - E_S$ (**2**) ≥ −1.3 kcal mol^{-1}. Thus, combining the upper and lower limits, we estimate that the singlet−triplet gap of **2** lies between 0.8 and 1.3 kcal mol^{-1}. Likewise, one can combine the lower limit of $E_T - E_S$ (**1**) ≥ 2.3 kcal mol^{-1} and $E_T - E_S$ (**2**) ≤ −0.8 kcal mol^{-1} with the calculated $\Delta\Delta E_{ST} = 3.6$ kcal mol^{-1} to estimate that the singlet−triplet gap of **1** lies between 2.3 and 2.8 kcal mol^{-1}.

Conclusions

Two Kekulé hydrocarbons, 2,2-dimethyl-2*H*-benzo[*cd*]fluoranthene (**1**) and its benzannellated analogue 2,2-dimethyl-2*H*-dibenzo[*cd*,*k*]fluoranthene (**2**), were generated photochemically from two different photoprecursors each and investigated spectroscopically in cryogenic matrices by UV−vis, fluorescence, and EPR and in solution using ns flash photolysis and chemical trapping experiments. Hydrocarbon **1** was found to be a ground-state singlet species, EPR-silent, with long-wavelength electronic absorptions ($\lambda_{max} = 1284$ nm) characteristic of quinonoidal species. Compound **2**, on the other hand, has a triplet ground state, the first such neutral Kekulé hydrocarbon. Its EPR spectrum ($|D/hc| = 0.0210$ cm^{-1}, $|E/hc| = 0.0034$ cm^{-1}) displays a linear Curie dependence, and its UV−vis and fluorescence spectra are similar to those of triplet 1,8-naphthoquinodimethanes. Density functional calculations on the demethylated analogues of **1** and **2** predicted a singlet ground state for the smaller system and a triplet ground state for the larger, in agreement with the experimental results. Using the results of the spectroscopic measurements, trapping experiments, and DFT calculations, the singlet−triplet gap for **1** is estimated to be 2.3−2.8 kcal mol^{-1}, with the singlet the ground state, and 0.8−1.3 kcal mol^{-1} for **2**, in favor of the triplet.

Experimental Section

Solvents and Matrix Materials. 2-Methyltetrahydrofuran (MTHF) was purchased from Fluka, distilled over Na, and stored degassed over Na/K alloy. It was then vacuum transferred immediately prior to use. 1-Pentanol (Fluka) was stored over molecular sieves and vacuum transferred for use. Dibutyl phthalate, methylcyclohexane, phenyl salicylate, and tetrakis(dimethylamino)ethylene were purchased from Fluka and used as received. Adamantane (Fluka) was purified by "ultra-flash" chromatography: the adamantane was dissolved in petroleum ether and suction filtered through 5 cm of silica gel in a fritted funnel, leaving the colored impurities at the head of the "column"; fresh petroleum ether was used to elute remaining adamantane from the silica gel.

UV/Vis and EPR Spectroscopy. Optical absorption spectra were obtained using a Perkin-Elmer Lambda 9 or Lambda 19 spectrometer and an Oxford 1704 cryostat with liquid nitrogen as cryogen. EPR spectra were acquired on a Bruker ESP-300 spectrometer. The cavity was equipped with a slotted front-plate for irradiation in the cavity. The light source was a 1000-W Hg(Xe) arc lamp (Hanovia 977-B1), the output of which was filtered by a water-cooled Schott UG-5 (2 mm thick) filter as well as additional filters as described in the text and focused into the cavity. Low temperatures were obtained with a flow of N_2 gas, generated by means of a heating coil inserted into a Dewar of liquid N_2 and led through a heat exchange coil submerged in liquid N_2 in a second Dewar. With this system, temperatures as low as ~89 K were attainable by setting the heating coil current to maximum.

(28) Downing, J.; Dvorak, V.; Kolc, J.; Manzara, A.; Michl, J. *Chem. Phys. Lett.* **1972**, *17*, 70−73.
(29) Snyder, G. J. Ph.D. Thesis, California Institute of Technology, 1988.
(30) Platz, M. S. In *Diradicals*; Borden, W. T., Ed.; Wiley: New York, 1982; pp 195−258.

Temperatures above 89 K were attained by a combination of: (a) decreasing the heating coil current in the Dewar and (b) heating the N_2 gas with a heater located below the cavity. Samples for EPR spectroscopy were placed in quartz tubes (5 mm OD, 3 mm ID, 25 cm long) which had been washed consecutively with 5% aqueous HF, H_2O, KOH/methanol, H_2O and acetone and dried under vacuum. The tubes were fashioned from Heraeus grade HSQ300 quartz tubing. Samples were degassed by three cycles of freeze−pump−thaw and then sealed while frozen under static vacuum.

For the Curie plot, Suprasil EPR tubes were obtained from Wilmad (4 mm OD, 2.4 mm ID, 25 cm long). EPR spectra were acquired using a Varian E9 spectrometer. The irradiation source was a 1000-W Hg(Xe) arc lamp, the output of which was focused directly into the cavity through a slotted front plate. Low temperatures were attained with an Oxford Instruments helium cryostat using liquid helium as cryogen. The temperature was measured using a gold−iron (0.07 atomic %) and chromel thermocouple which was located near the He nozzle, approximately 1 cm below the sample, and indicated on the Oxford ITC instrument. Calibration experiments using an external thermocouple within the sample indicated a temperature deviation between the ITC and sample of approximately 1 K. Temperature control was attained by a combination of manual adjustment of the He flow and automatic adjustment of a heating coil (wrapped noninductively around the He nozzle) by the ITC. Spectra were analyzed and integrated using the program "ESR7", developed by Dr. Ulrich Walther, Männedorf. The sample was irradiated at 75 K for 5 min with the unfiltered output of the Hg(Xe) arc lamp, operated at 150 W. After irradiation, the slotted front plate was replaced with a solid plate to avoid further irradiation from stray room light. EPR spectra were acquired at 0.01 mW microwave power (the lowest value at which the signal was stable) and 10 G modulation amplitude. After each temperature change, the sample was allowed around three minutes to equilibrate. Control experiments showed no change in the spectra after longer equilibration times. The data were acquired decreasing the temperature from 75 to 4 K, then increasing back to 75 K. No significant difference was observed in the two sets of data.

Preparation of Samples for High-Temperature Matrix EPR Spectroscopy. Poly(methyl methacrylate) (PMMA): Cyclopropane **3** was embedded in PMMA as follows: solid PMMA powder was first dissolved in CH_2Cl_2, after which a CH_2Cl_2 solution of the cyclopropane was added. The viscous solution was mixed thoroughly and then spread onto a glass plate. The methylene chloride was removed by a stream of N_2 directed over the plate. After the film was free of solvent, it was peeled off the glass plate, rolled up and inserted into a quartz EPR tube. This was degassed under high vacuum at room temperature and sealed. Adamantane: Diradical **1** was generated in adamantane matrices from both cyclopropane **3** as well as dibromide **4**. In the case of the cyclopropane, a CH_2Cl_2 solution of **3** was added to a solution of adamantane in petroleum ether. Solvent was removed quickly using the rotary evaporator. The adamantane was transferred to an EPR tube and degassed at room temperature to a pressure of approximately 0.2 Torr, corresponding to the vapor pressure of adamantane, and sealed. In the case of the dibromide, a solution of adamantane, **4**, and TDAE was similarly concentrated in vacuo, transferred to an EPR tube, degassed and sealed. Phenyl salicylate: A solution of **3** in a few drops CH_2Cl_2 was added to an EPR tube, and the solvent removed in vacuo. Solid, crystalline phenyl salicylate was then added to the tube. The tube was degassed under dynamic vacuum at room temperature and sealed. The tube was then placed in a 50 °C water bath, upon which the phenyl salicylate melted, dissolving the cyclopropane. Although the solution had a tendency to crystallize upon standing, by warming the sample shortly before freezing it, a relatively clear glass could be formed. Dibutyl phthalate: Solid **3** was taken up in dibutyl phthalate, transferred to an EPR tube, degassed and sealed. Due to the solvent's high viscosity, special care must be taken during degassing to avoid gas bubbles from pushing the solution out of the tube.

Fluorescence Spectroscopy. Fluorescence excitation and emission spectra were obtained with a Spex Fluorolog spectrometer, using a Hamamatsu R928 photomultiplier. Emission spectra were corrected for photomultiplier sensitivity out to 800 nm. Both emission and excitation spectra were taken in units of counts-per-wavelength and converted to counts-per-wavenumber using a λ-squared correction.

Spectroscopy of Oriented Samples. Sheets of polyethylene (∼3 × 3 cm) were loaded with the compound of interest by swelling the sheet in a chloroform solution of the compound. After swelling, the sheets were rinsed with methanol to free the surface of particles and microcrystals, which could compromise the polarization of incident light. The sheets were clamped into a stretching device and stretched to a three- to 4-fold increase in length. While still held stretched, the sheets were mounted onto a small, metal mount equipped with a long metal shaft. The sample was then lowered into the Oxford cryostat, which was mounted into the path of the spectrometer.

The Perkin-Elmer Lambda 9 spectrometer was found to have considerable polarization even in the absence of an orienting sample. This polarization varied considerably with wavelength, and reached a maximum of over 90% around 500 nm and at 860 nm, where the detector changes. Thus, a Hanle-type wedge depolarizer (Halle Optik, Berlin) was used to remove this instrumental polarization. The depolarizer reduces the instrumental polarization to approximately 2% throughout the NIR, and less than 5% in the visible. The residual polarization increases somewhat below 250 nm, where the polarizer begins to absorb significantly.

Nanosecond Laser Flash Photolysis. The apparatus used for kinetic and spectrographic ns flash photolysis has been described in detail elsewhere.[16] The measurements described herein utilized a mirrored cell holder.[31] The laser source was a Lambda Physik COMPex excimer laser (248 or 351 nm). Solutions for flash photolysis were degassed by three cycles of freeze−pump−thaw.

Acknowledgment. This work was funded by the Swiss National Science Foundation and by the Petroleum Research Fund, administered by the American Chemical Society. We thank A. Liégard and Dr. G. Rist of Novartis AG, Basel, for collaborating on the Curie plot.

Supporting Information Available: Experimental details (PDF). This material is available free of charge via the Internet at http://pubs.acs.org.

JA0004377

(31) Bonneau, R.; Wirz, J.; Zuberbühler, A. D. *Pure Appl. Chem.* **1997**, *69*, 979−992.